

Supplement of Ocean Sci., 13, 983–995, 2017
<https://doi.org/10.5194/os-13-983-2017-supplement>
© Author(s) 2017. This work is distributed under
the Creative Commons Attribution 4.0 License.



Supplement of

**Combining physical and geochemical methods to investigate
lower halocline water formation and modification
along the Siberian continental slope**

Matthew B. Alkire et al.

Correspondence to: Matthew B. Alkire (malkire@apl.washington.edu)

The copyright of individual parts of the supplement might differ from the CC BY 4.0 License.

Contents of this file

Text S1 to S2
Tables S1 to S4
Figures S1 to S4

Introduction

The following supporting information includes text describing the instruments and methods used for data collection (Text S1) and the water type analysis used to estimate fractional contributions of meteoric water, net sea-ice meltwater, and Atlantic water to each discrete water sample collected during the 2013 and 2015 cruises (Text S2). Table S1 summarizes the winter mixed layer depths and estimates of the mean salinities and potential temperatures of the subsequent winter mixed layer. Additional tables summarize linear regressions of salinity and stable oxygen isotope ratio ($\delta^{18}\text{O}$) data in specified salinity ranges from the 2015 cruise (Tables S2 and S3) and additional data sets for comparison (Table S4). Figure S1 provides a schematic of salinity and $\delta^{18}\text{O}$ changes that take place during the transition of halocline waters from the sea-ice melt branch mixing regime to the meteoric water branches as a result of mixing with overlying freshwaters, brine expulsion during ice formation, and mixing with underlying Atlantic waters. Figure S2 compares the salinity and $\delta^{18}\text{O}$ data collected during the 2013 cruise data and used to define mixing relationships in the salinity range $34 \leq S < 34.5$ against the salinity and $\delta^{18}\text{O}$ characteristics of lower halocline water types defined by *Bauch et al.*, [2016]. Figures S3 and S4 provide vertical profiles of potential temperature and salinity from selected stations occupied during the 2013 cruise.

Text S1. Full description of instrumentation and water sampling methods employed during the 2013 and 2015 cruises.

The sensor suite utilized during the 2013 and 2015 cruises included a Seabird SBE9*plus* conductivity-temperature-depth (CTD) equipped with dual temperature (SBE3), conductivity (SBE4), and dissolved oxygen (SBE43) sensors, SBE5T submersible pump, and a digi-quartz pressure sensor. Additional channels of the CTD system were directly connected to external sensors mounted on the carousel, including a WET Labs ECO-FLNTU chlorophyll and turbidity sensor, a WET Labs C-Star transmissometer (beam transmission and attenuation), a photosynthetically-active radiation (PAR) sensor (Biospherical model QCP2350), and a Satlantic Deep Submersible Ultraviolet Nitrate Analyzer (SUNA). A Benthos PSA-916 altimeter was also mounted to the bottom of the rosette to avoid hitting the carousel on the seafloor. Finally, twenty-four Niskin bottles (10 L capacity) were included for the collection of water samples at specified depths. All instruments were levelly mounted in the bottom section of the carousel directly below the Niskin bottles. Data was monitored and acquired during each cast using a Seabird SBE11*plus* Deck Unit.

During each cast, the rosette was moved outside to the starboard (2013) or port side (2015) deck from either a warmed container on deck using a wheeled cart (2013) or from the hydrology lab inside the ship using a hydraulic crane (2015). The rosette was then transferred to a winch and lowered over the side of the vessel to a depth of ~15 m for initialization and sensor equilibration. The rosette was then brought up to the surface (0-3 m) and then lowered through the water column at a relatively constant rate to a depth of either ~1000 m or between 5 and 20 m above the bottom (most casts were conducted to ~1000 m as some instruments cannot withstand pressures exceeding 1000 db). Once the maximum depth was reached, the rosette was stopped and a Niskin bottle was fired to obtain a water sample. The rosette was then brought back up through the water column and routinely stopped at depths of 500, 250, 200, 150, 140, 130, 120, 110, 100, 90, 80, 70, 60, 50, 40, 30, 20, 10, and 2-4 m (surface) for the collection of water samples (alternate or additional depths were tripped on a cast-by-cast basis). The rosette was stopped for a period of ~30 seconds before sample collection to allow the bottles to soak and minimize turbulent flows caused the carousel's wake as it moved upward through the water column. Once the rosette reached the surface, it was brought back on deck and transferred inside the hydrology lab using the crane.

Salinity samples were collected into 125-mL glass bottles equipped with polyethylene inserts to prevent evaporation. In 2013, salinity samples were analyzed via salinometer onboard after a 12-hour temperature equilibration. However, unstable laboratory temperatures prevented the collection of quality data from the salinometer; thus, the bottle salinity data was not utilized from the 2013 cruise. In 2015, bottle samples ($n = 93$) for salinity determinations were collected and shipped back to the University of Washington for analysis using a Guideline 8400B salinometer (calibrated with IAPSO standard seawater) at the Marine Chemistry Laboratory (UW Oceanography). The majority (76 %) of bottle salinities differed from CTD salinities by ≤ 0.04 , though larger discrepancies did occur (49 % of available comparisons indicated differences of ≤ 0.01 and 86 % indicated differences ≤ 0.1).

Text S2: Full description of water type analysis methods.

Fractional contributions of meteoric water (MW) and net sea-ice meltwater (SIM), and a saline water endmember (Atlantic seawater, AW, for the purposes of this study) can be quantified using salinity and $\delta^{18}\text{O}$ observations in a set of coupled equations that also conserves mass (or volume):

$$S_{\text{SIM}} \times f_{\text{SIM}} + S_{\text{MW}} \times f_{\text{MW}} + S_{\text{AW}} \times f_{\text{AW}} = S_{\text{obs}} \quad (1)$$

$$\delta^{18}\text{O}_{\text{SIM}} \times f_{\text{SIM}} + \delta^{18}\text{O}_{\text{MW}} \times f_{\text{MW}} + \delta^{18}\text{O}_{\text{AW}} \times f_{\text{AW}} = \delta^{18}\text{O}_{\text{obs}} \quad (2)$$

$$f_{\text{SIM}} + f_{\text{MW}} + f_{\text{AW}} = 1 \quad (3)$$

where f equals the fractional contributions of the three water types (i.e., SIM, MW, and AW) and S and $\delta^{18}\text{O}$ represent the characteristic salinities and stable oxygen isotopic ratios associated with these water types. Note that net sea-ice formation (formation exceeding melting) will generate a negative SIM fraction ($f_{\text{SIM}} < 0$), representing an extraction of liquid water into the solid phase (ice) and the release of brine into the water column. This water type analysis assumes that salinity and $\delta^{18}\text{O}$ values that characterize MW, SIM, and AW (commonly referred to as endmember values) are well known and relatively stable over time. However, there is seasonal and interannual variability associated with these endmember values that should be taken into account when conducting a water type analysis. Thus, estimates of uncertainty in the water type fractions resulting from the analysis can be computed by varying the endmember values within reasonable ranges of natural variability. In this study, meteoric water $\delta^{18}\text{O}$ endmember values were varied between -22 and -18 ‰. The salinity of meteoric water is zero by definition. Sea-ice meltwater salinity and $\delta^{18}\text{O}$ endmember values were varied between 2 and 8 and -2 and +3 ‰, respectively. Atlantic seawater salinity and $\delta^{18}\text{O}$ endmember values were varied between 34.85 and 35 and 0.25 and 0.35 ‰, respectively.

Similar to the methods described in *Alkire et al.* [2015], the water type analysis was iterated 1,000 times for each salinity and $\delta^{18}\text{O}$ pair. The set of endmember values characterizing MW, SIM, and AW were randomly selected from the specified ranges for each iteration. Though the endmember selection was randomized, it was organized in such a way that allowed all values within each range to be selected an equal number of times. Averages of the MW, SIM, and AW fractions (1,000 values for each salinity, $\delta^{18}\text{O}$ pair) were taken as the best estimate of the water type fractions and associated standard deviations taken as estimates of uncertainties due to natural variations in the endmember assignments. The median standard deviations for MW, SIM, and AW fractions were 0.24, 0.36, and 0.20 % for the 2013 cruise and 0.29, 0.41, and 0.21 % for the 2015 cruise, respectively. Note that these uncertainties are *absolute* uncertainties (e.g., meteoric water fraction reported as 8 ± 0.24 %).

Table S1. Winter mixed layer (WML) depth, salinity, and potential temperature (θ) estimated from CTD data by identifying the minimum potential temperature below the surface mixed layer. We note that the identification of the WML depth by this method is associated with some uncertainty and may be particularly ambiguous at stations with a mixed layer close to the freezing point. The WML depths estimated using this method were visually checked against vertical profiles of potential temperature and θ -S diagrams. Stations that appeared to have no clearly identifiable θ_{\min} or multiple minima are marked with “*CND*” (could not determine). “Salt mixed” and “ θ mixed” refer to the mean salinities and potential temperatures estimated from individual profiles assuming the water column will be homogenized down to the previous year’s WML.

Station	Transect	WML Depth (m)	WML Salinity	WML θ	Salt mixed	θ mixed
1	-	52	34.556	-0.699	34.112	1.009
2	-	56	34.368	-1.674	33.867	-1.317
3	-	45	34.365	-1.384	33.876	-1.277
4	-	52	34.414	-1.533	33.849	-1.501
5	-	49	34.443	-1.485	33.563	-1.240
6	-	48	34.236	-1.663	32.940	-0.403
7	L5	<i>CND</i>	-	-	-	-
8	L5	<i>CND</i>	-	-	-	-
9	L5	85	34.282	-1.659	33.084	-0.417
10	L5	87	34.317	-1.611	33.350	-0.631
11	L5	58	34.024	-1.750	32.457	-0.503
12	L5	50	33.893	-1.792	32.896	-1.097
13	L5	64	33.896	-1.799	32.744	-1.272
14	L5	56	33.918	-1.797	32.947	-1.486
15	L5	52	34.023	-1.775	33.315	-1.611
16	L5	67	34.210	-1.727	33.573	-1.667
17	L5	53	33.968	-1.762	33.141	-1.653
18	L5	52	34.149	-1.721	33.285	-1.589
19	L5	40	33.995	-1.733	33.098	-1.622
20	L5	42	34.011	-1.747	32.939	-1.611
21	L5	59	33.994	-1.745	33.076	-1.622
22	L5	45	33.720	-1.730	32.331	-1.577
23	L5	55	33.934	-1.754	32.526	-1.627
24	L5	39	33.383	-1.770	32.022	-1.610
25	L5	68	33.838	-1.819	32.630	-1.671
26	L5	47	33.464	-1.759	31.888	-1.611
27	-	<i>CND</i>	-	-	-	-
28	-	<i>CND</i>	-	-	-	-
29	L6	70	34.022	-1.675	31.551	-1.127
30	L6	70	34.056	-1.633	31.863	-1.348
31	L6	61	33.801	-1.655	31.125	-1.320
32	L6	73	34.006	-1.664	31.556	-1.482

33	L6	51	33.513	-1.717	31.162	-1.434
34	L6	46	32.992	-1.675	30.677	-1.489
35	L6	40	32.340	-1.620	30.412	-1.468
36	L6	44	33.242	-1.739	30.896	-1.532
37	L6	46	32.973	-1.731	31.124	-1.603
38	L6	75	34.020	-1.706	32.116	-1.597
39	-	59	33.150	-1.753	32.020	-1.659
40	-	44	32.557	-1.673	30.467	-1.254
41	-	46	32.484	-1.742	31.099	-1.620
42	-	39	32.494	-1.712	31.246	-1.651
43	-	37	32.202	-1.679	31.044	-1.652
44	-	52	32.384	-1.693	31.357	-1.668
45	L5.5	43	33.180	-1.600	30.802	-0.745
46	L5.5	51	33.897	-1.659	31.681	-0.435
47	L5.5	CND	-	-	-	-
48	L5.5	48	33.980	-1.683	32.122	-0.542
49	L5.5	63	34.234	-1.571	32.615	-0.603
50	L5.5	58	34.204	-1.591	32.590	-0.622
51	L5.5	CND	-	-	-	-
52	L5.5	CND	-	-	-	-
53	L5.5	CND	-	-	-	-
54	L5.5	CND	-	-	-	-
55	L5.5	CND	-	-	-	-
56	L5.5	50	33.867	-1.776	32.323	-1.124
57	L5.5	59	33.921	-1.774	32.931	-1.100
58	L5.5	63	33.961	-1.766	32.750	-0.674
59	-	65	34.051	-1.728	33.112	-0.711
60	L5	62	33.986	-1.762	32.831	-0.674
61	L5	44	33.991	-1.728	33.177	-1.271
62	L5	44	34.000	-1.737	33.045	-1.000
63	L4	CND	-	-	-	-
64	L4	CND	-	-	-	-
65	L4	26	33.959	-1.670	32.814	-1.067
66	L4	CND	-	-	-	-
67	L4	42	34.297	-1.688	33.673	-1.421
68	L4	51	34.334	-1.689	33.783	-1.381
69	L4	46	34.353	-1.716	33.739	-1.404
70	L3	20	32.257	-1.718	32.246	-1.714
71	L3	15	31.864	-1.718	31.864	-1.719
72	L3	CND	-	-	-	-
73	L3	CND	-	-	-	-
74	L3	31	33.955	-1.686	33.097	-1.588
75	L3	22	34.040	-1.683	33.327	-1.517

76	L3	33	34.195	-1.663	33.208	-1.602
77	L3	48	34.322	-1.681	33.715	-1.560
78	L3	52	34.354	-1.610	33.692	-1.441
79	L3	CND	-	-	-	-
80	L3	CND	-	-	-	-
81	L3	CND	-	-	-	-
82	L2	CND	-	-	-	-
83	L2	CND	-	-	-	-
84	L2	CND	-	-	-	-
85	L2	54	34.309	-1.385	33.709	-0.538
86	L2	53	34.336	-1.566	33.798	-0.783
87	L2	42	34.370	-1.545	33.711	-0.567
88	L2	55	34.360	-1.584	33.799	-0.664
89	L2	51	34.392	-1.623	33.825	-0.995
90	L2	52	34.390	-1.694	33.893	-1.255
91	L2	58	34.405	-1.723	33.800	-1.410
92	L2	CND	-	-	-	-
93	L2	51	34.393	-1.648	33.823	-1.166
94	-	87	34.420	-1.770	34.014	-1.624
95	-	44	33.993	-1.727	32.937	-1.689
96	-	CND	-	-	-	-
97	L1	CND	-	-	-	-
98	L1	CND	-	-	-	-
99	L1	85	34.366	-1.795	33.925	-1.647
100	L1	CND	-	-	-	-
101	L1	71	34.370	-1.764	34.050	-1.601
102	L1	58	34.367	-1.719	34.004	-1.460
103	L1	58	34.372	-1.710	33.861	-1.332
104	L1	66	34.390	-1.705	33.995	-1.409
105	L1	59	34.379	-1.728	33.942	-1.337
106	L1	30	34.363	-1.547	33.654	-0.659
107	L1	45	34.289	-1.610	33.781	-0.443
108	L1	45	34.292	-1.589	33.737	-0.198
109	SAT	CND	-	-	-	-
110	SAT	CND	-	-	-	-
111	SAT	48	34.626	-0.168	34.309	1.795
112	SAT	43	34.583	-0.213	34.245	1.788
113	SAT	42	34.526	-0.535	34.010	1.085
114	SAT	38	34.337	-1.411	33.769	-0.176
115	SAT	35	34.274	-1.355	33.708	0.080
116	SAT	39	34.322	-1.321	33.626	0.141

Averages

ALL stations	51	33.932	-1.617	32.890	-1.085
SIM Branch stations	50	34.370	-1.475	33.825	-0.719

Table S2. Linear regression analyses (restricted to salinities ≥ 34.5) of salinity- $\delta^{18}\text{O}$ measurements collected along transects occupied during the 2015. Slopes, intercepts, correlation coefficients (r) and associated standard errors (se) are reported for each transect.

Transect	Slope	se	Intercept	se	Corrcoeff	Stations
SAT	0.2243	0.0723	-7.5502	2.5162	0.299	81-93
L2	0.4317	0.0418	-14.8127	1.4567	0.7723	2-9 & 78-79
L5	0.6056	0.0345	-20.8911	1.1974	0.8454	10-24 & 72-76
L6	0.572	0.0436	-19.7179	1.5128	0.8763	27-38
165E	0.7238	0.147	-24.9681	5.1044	0.7017	39-54
175E	0.5906	0.104	-20.3403	3.6086	0.6777	56-71

Table S3. Linear regression analyses (restricted to the salinity range: $34 \leq S < 34.5$) of salinity- $\delta^{18}\text{O}$ measurements collected along transects occupied during the 2015. Slopes, intercepts, correlation coefficients (r) and associated standard errors (se) are reported for each transect.

Transect	Slope	se	Intercept	se	Corrcoeff	Stations
SAT	0.3252	0.1944	-11.0302	6.6668	0.5092	81-93
L2	0.3292	0.0839	-11.2715	2.8837	0.5887	2-9 & 78-79
L5	1.556	0.107	-53.6881	3.6745	0.8267	10-24 & 72-76
L6	1.3081	0.0716	-45.0777	2.4549	0.9048	27-38
165E	0.8079	0.0824	-27.9041	2.8254	0.8499	39-54
175E	1.1662	0.0746	-40.239	2.5568	0.9472	56-71

Table S4. Linear regression analyses of salinity- $\delta^{18}\text{O}$ measurements available from different data sets, including the North Pole Environmental Observatory (NPEO) [Alkire *et al.*, 2015], Global Seawater Oxygen-18 Database [Schmidt *et al.*, 1999], and *Polarstern* cruise ARK-XXI/2 [Bauch *et al.*, 2011]. Slopes, intercepts, and correlation coefficients are reported for each data set. NPEO data were collected annually between 2000 and 2015 (no data from 2009) at latitudes $\geq 85^\circ\text{N}$, primarily along longitudinal transects 90°E and 180° [Alkire *et al.*, 2015]. Measurements from the O-18 Database were restricted to latitudes $\geq 75^\circ\text{N}$, and longitudes ranging between 65 and 160°E to best resemble the area studied in 2013. Further restrictions were applied, limiting the O-18 data to years after 2000 (2000, 2001, 2007, 2008) and then to 2007-2008, to determine the impact (if any) on $\delta^{18}\text{O}$ -S relationships. ARK-XXII/2 data were similarly restricted to latitudes $\geq 75^\circ\text{N}$ and longitudes 65 - 160°E . A second longitudinal restriction (110 - 160°E) was employed on the ARK-XXII/2 data to investigate the spatial dependence on the regression coefficients.

Data Source	Years	Salinity Range	Slope	Intercept	Corrcoef	N
NPEO	2000-2015	$S \geq 34.5$	0.6690	-23.1220	0.7877	141
		$34 \leq S < 34.5$	1.1423	-39.4408	0.6305	162
O-18 Database	1967-2008	$S \geq 34.5$	0.4618	-15.8776	0.5191	1350
		$34 \leq S < 34.5$	0.8635	-29.7775	0.6524	304
	2000-2008	$S \geq 34.5$	0.5401	-18.5999	0.6571	606
		$34 \leq S < 34.5$	0.9234	-31.8298	0.6757	153
	2007-2008	$S \geq 34.5$	0.6261	-21.5984	0.7091	598
		$34 \leq S < 34.5$	0.9669	-33.3287	0.7621	125
ARK-XXII/2	2007	$S \geq 34.5$	0.3749	-12.9036	0.5923	104
		$34 \leq S < 34.5$	0.2478	-8.6570	0.2219	113
	110-160°E	$S \geq 34.5$	0.3796	-13.1062	0.4748	24
	110-160°E	$34 \leq S < 34.5$	0.5205	-18.0897	0.5868	59

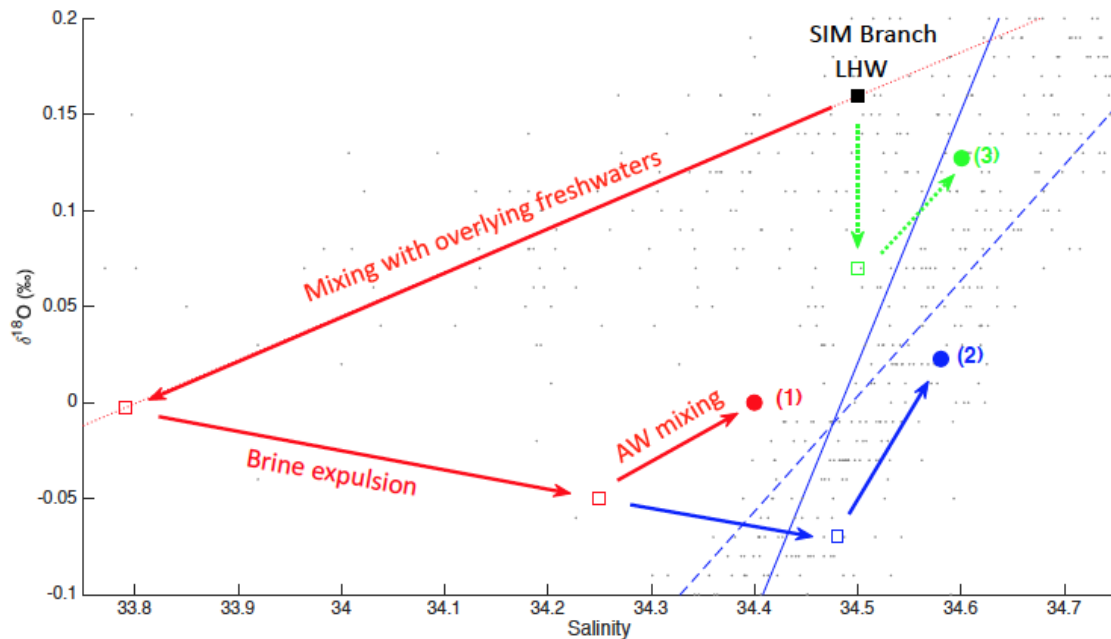


Figure S1. Schematic of the transition of lower halocline waters from the SIM branch to the MW branch via mixing with overlying freshwaters, salinization through sea ice formation/brine release, and mixing with Atlantic waters (AW). The red pathway illustrates the effect of vertical mixing down to 50 m (the mean winter mixed layer depth at SIM branch stations), brine expulsion due to the formation of 1 m of sea ice, and mixing with AW in a 21:79 ratio to form lower halocline water with a salinity of 34.4 and $\delta^{18}\text{O}$ of 0 ‰ (1). The blue pathway deviates from the red pathway due to additional ice formation (1.5 m instead of 1 m) to form lower halocline water with a salinity of 34.58 and $\delta^{18}\text{O}$ of 0.02 ‰ (2). The green pathway illustrates the effect of vertical mixing to 100 m, 1 m of sea ice formation, and AW mixing to form lower halocline water with a salinity of 34.6 and $\delta^{18}\text{O}$ of 0.13 ‰ (3). The regression lines representing the SIM branch (red, dotted line), upper MW branch (blue, dashed line), and lower MW branch (blue, solid line) are also shown for reference. The gray dots indicate data collected during the 2013 cruise. Empty squares indicate transition points after each step (freshwater mixing, brine expulsion, and AW mixing) whereas filled circles indicate the final halocline water product formed by the three potential pathways. All three pathways yield salinity and $\delta^{18}\text{O}$ combinations near (but not directly on) the MW mixing branches, indicating some additional processes and/or mixing (such as freshwater influence from river runoff) takes place during the transition from the SIM branch to the MW branch.

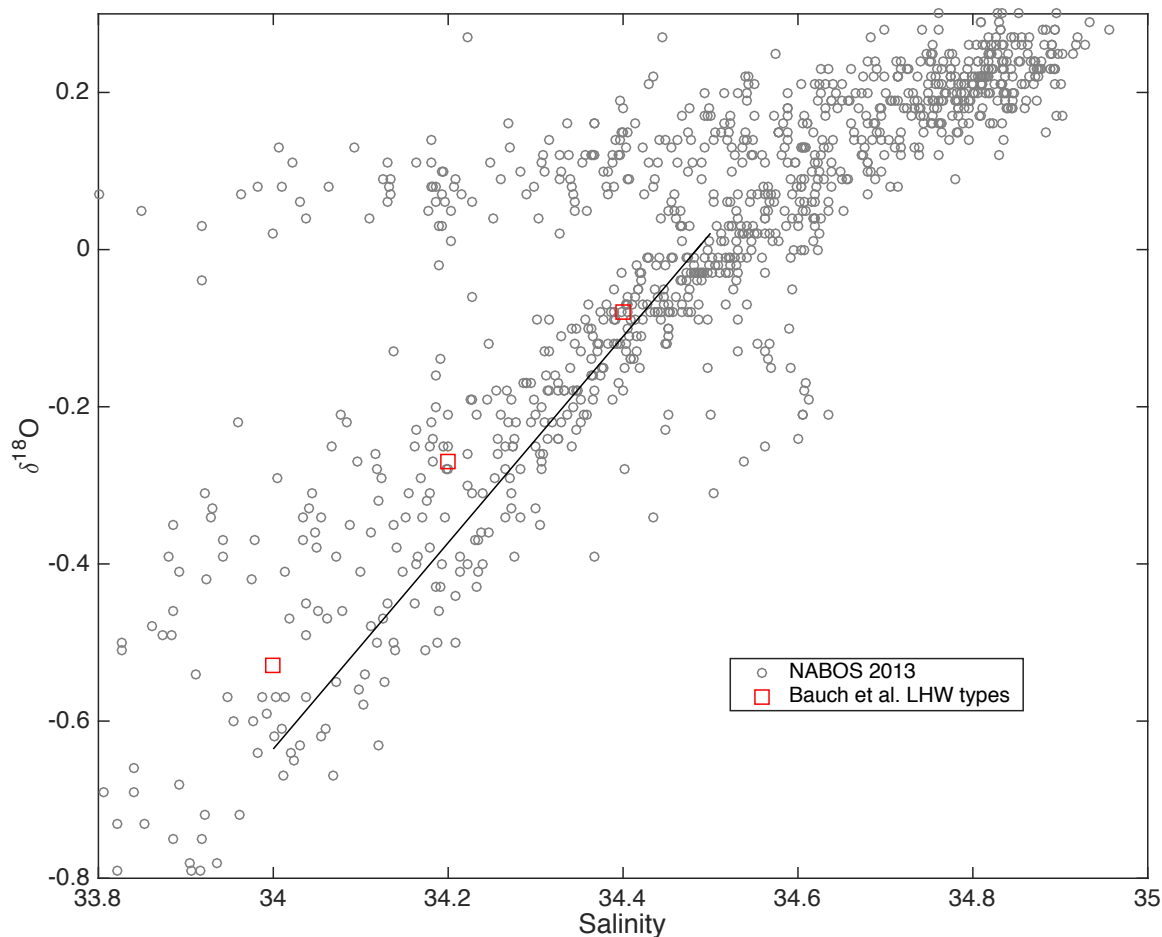


Figure S2. Plots of salinity versus the stable oxygen isotopic ratio ($\delta^{18}\text{O}$) measured during the 2013 cruise (gray circles) and characteristic values for the c2 ($S = 34$, $\delta^{18}\text{O} = -0.53\text{‰}$), c3 ($S = 34.2$, $\delta^{18}\text{O} = -0.27\text{‰}$), and c4 ($S = 34.4$, $\delta^{18}\text{O} = -0.08\text{‰}$) lower halocline water (LHW) water types (red squares) defined in *Bauch et al.* [2016]. The c1 LHW type ($S = 33.0$, $\delta^{18}\text{O} = -1.46\text{‰}$) is not shown. The linear regression defining the lower MW branch ($\delta^{18}\text{O} = 1.3126*S - 45.2639$) is included as a black, solid line. Note that a separate linear regression of the values characterizing the four LHW types was $\delta^{18}\text{O} = 0.9828*S - 33.901$.

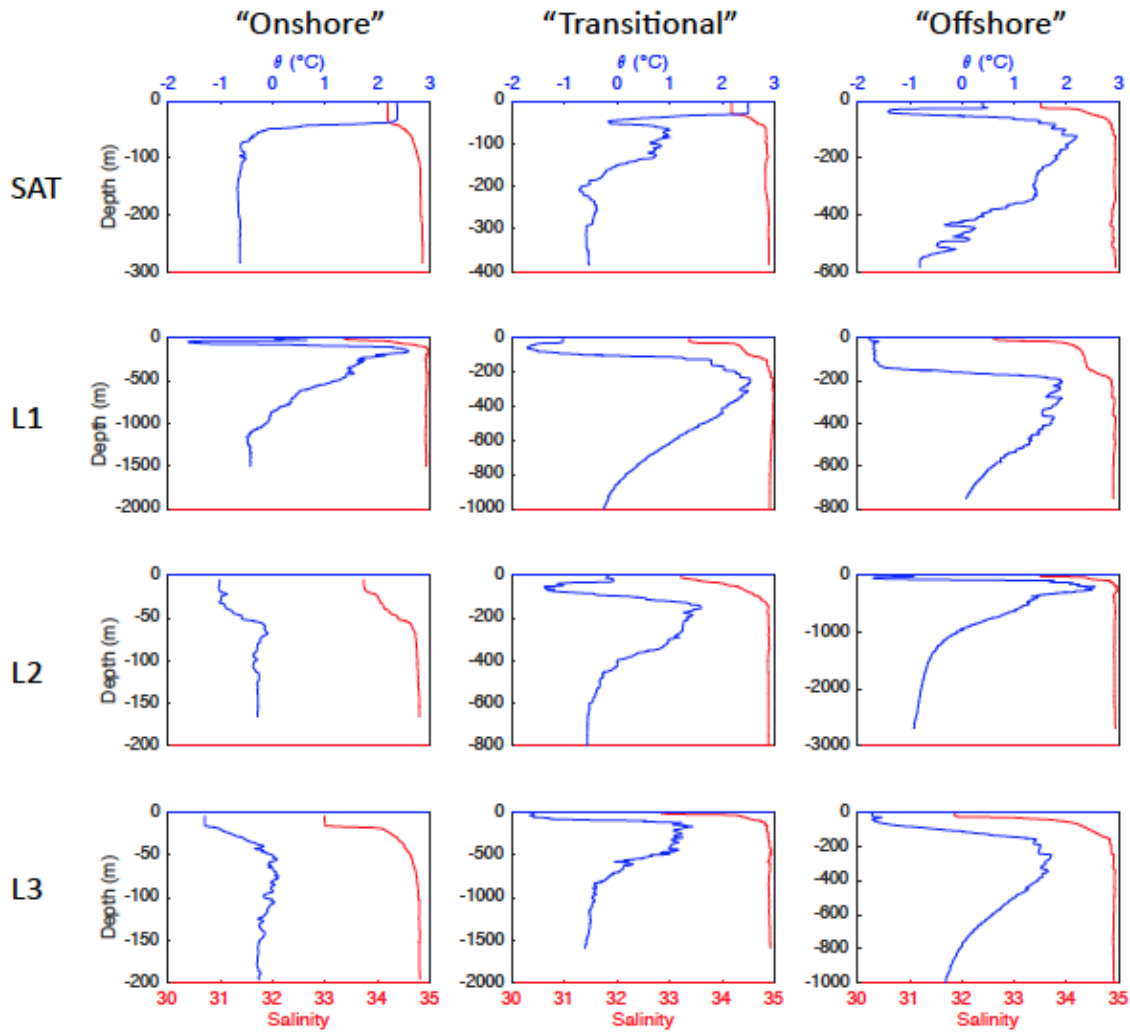


Figure S3. Vertical profiles of potential temperature (θ) and salinity plotted as blue and red lines, respectively, for selected stations on the SAT, L1, L2, and L3 transects. Stations were selected that generally represented the hydrographic conditions observed nearest the continental shelves (“onshore”), on the slope (“transitional”), and in the deep basins (offshore) along each transect. Note that, while the temperature and salinity axes are identical among panels, the range of the y-axes (depth) varies with each panel.

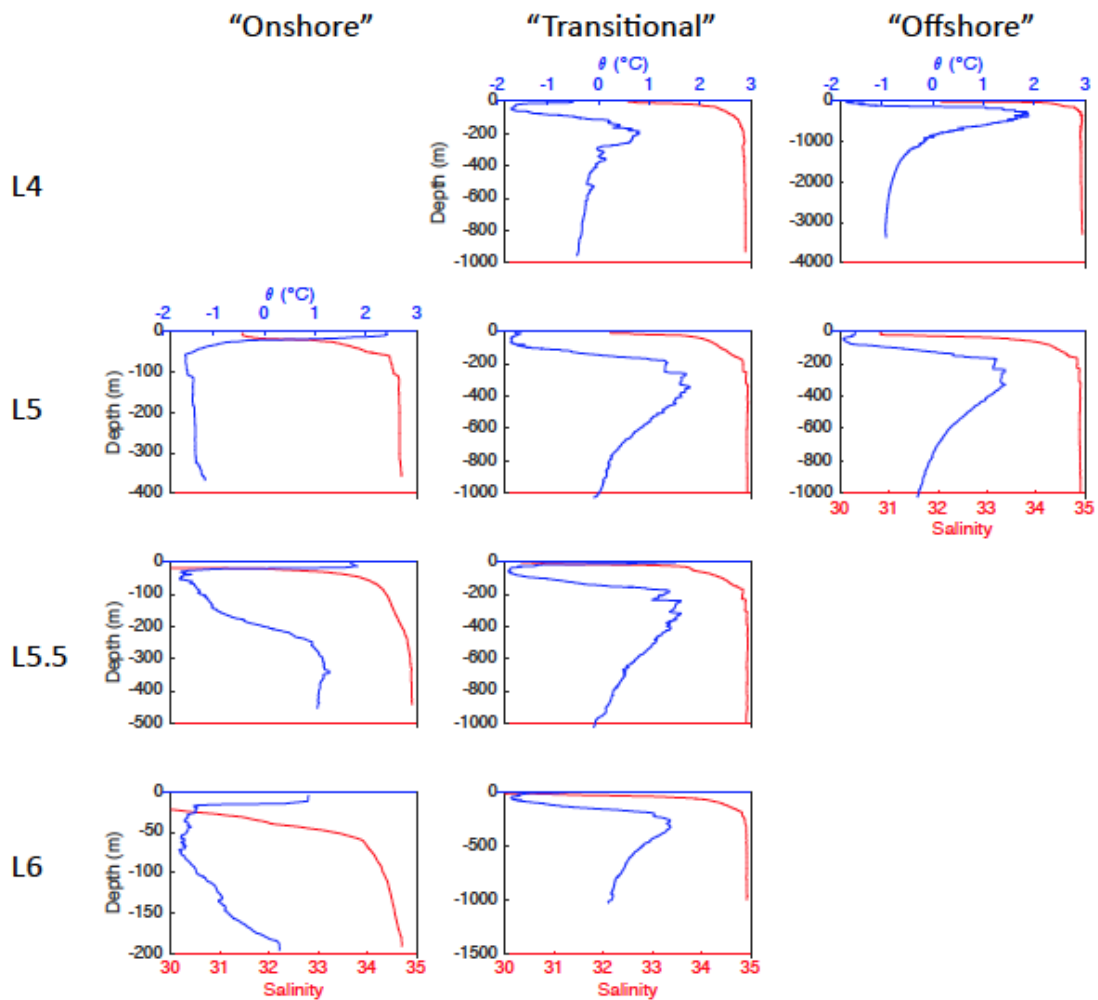


Figure S4. Vertical profiles of potential temperature (θ) and salinity plotted as blue and red lines, respectively, for selected stations on the L4, L5, L5.5, and L6 transects. Stations were selected that generally represented the hydrographic conditions observed nearest the continental shelves (“onshore”), on the slope (“transitional”), and in the deep basins (offshore) along each transect. Note that, while the temperature and salinity axes are identical among panels, the range of the y-axes (depth) varies with each panel.